Supplementary Materials: Hydrogen Solubility in FeSi Alloy Phases at High Pressures and Temperatures

Suyu Fu[1,*], Stella Chariton[2], Vitali B. Prakapenka[2], Andrew Chizmeshya[3], Sang-Heon Shim[1,*]

[1]School of Earth and Space Exploration, Arizona State University, Tempe, Arizona, USA.
[2]Center for Advanced Radiation Sources, University of Chicago, Chicago, Illinois, USA.
[3]School of Molecular Sciences, Arizona State University, Tempe, Arizona, USA.

Contents of this file

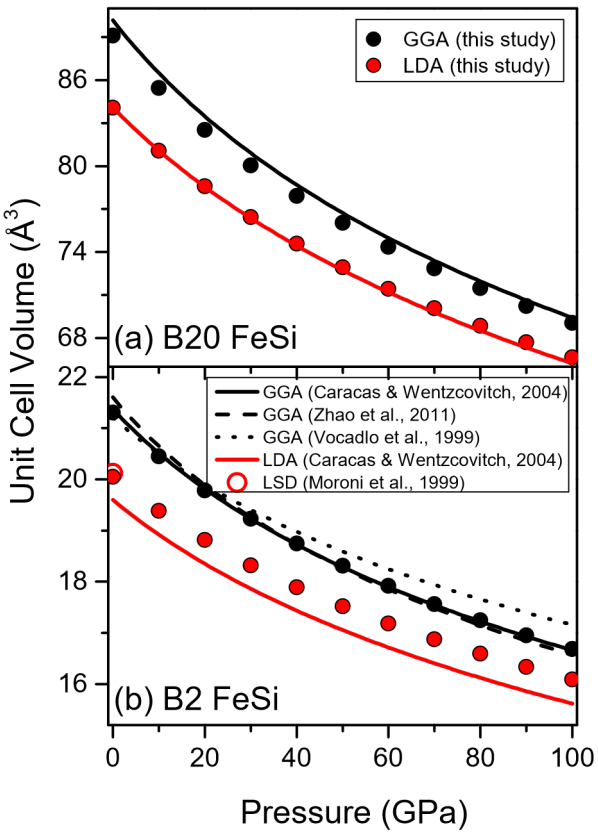

Figure S1: The unit-cell volumes of (**a**) B20 FeSi and **(b**) B2 FeSi from the DFT calculations. The solid black and red circles are from the GGA and LDA calculations, respectively, in this study. The curves are calculations from the literature (Caracas and Wentzcovitch, 2004; Moroni et al., 1999; Vocadlo et al., 1999; Zhao et al., 2011). The open red circle is calculated by Moroni et al. (1999) using a local-spin-density approximation.

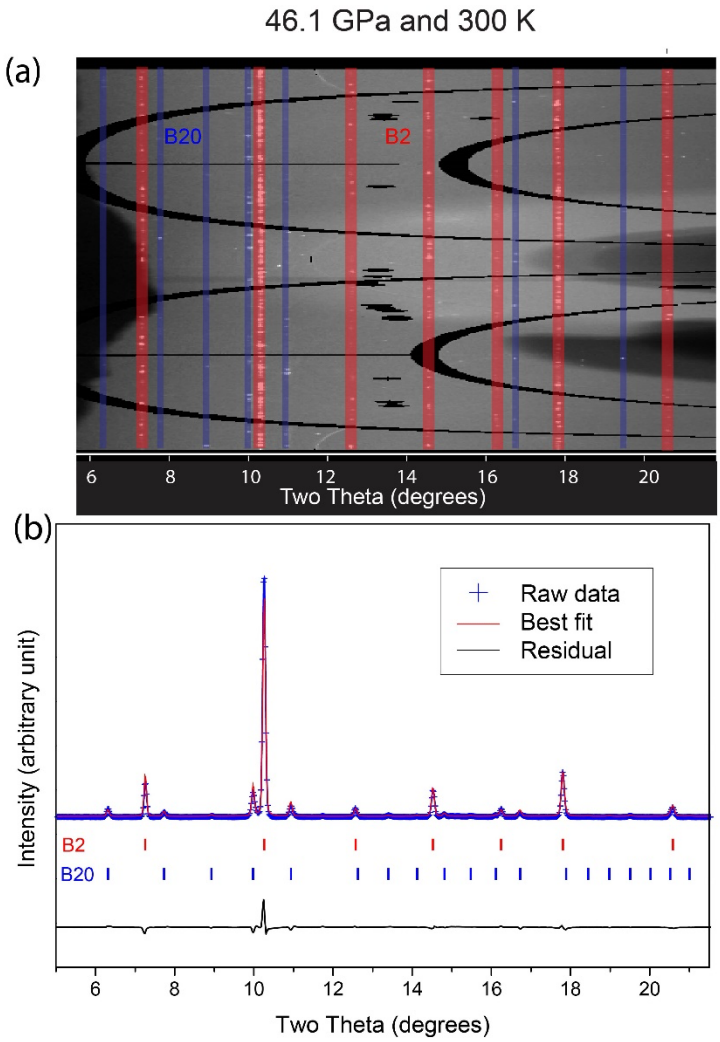

Figure S2: Rietveld refinement on a XRD pattern of the synthesized products at 46.1 GPa and 300 K. (**a**) Unrolled two-dimensional diffraction image. Diffraction peaks belonging to the B20 and B2 phases are highlighted with the blue and red boxes, respectively. (**b**) The best-fit result to the integrated pattern using GSAS-II. Both the B2 and B20 phases exist, indicated by the blue and red ticks, respectively. B2 is the predominant phase, about 95.6%, derived from the best fit. The spotty diffraction rings in the 2D image show that the sample was well heated and consequently recrystallized and stress-relaxed sufficiently.

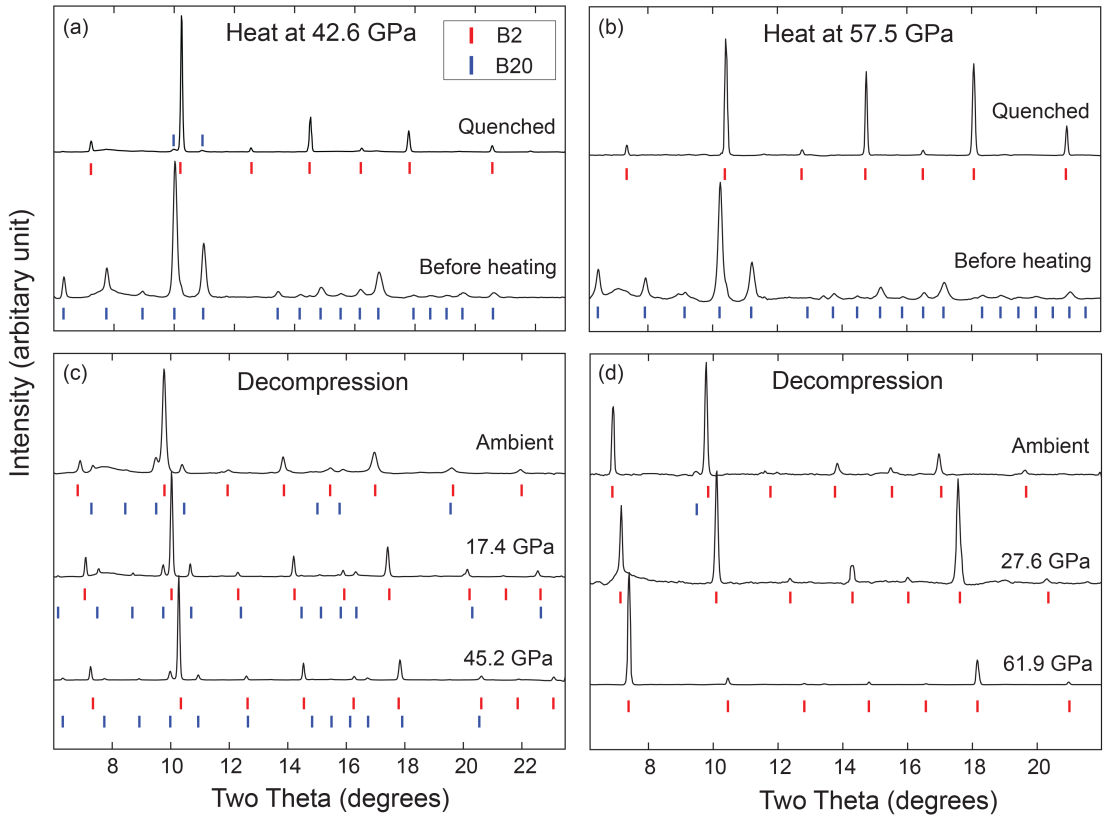

Figure S3: X-ray diffraction patterns of the synthesized B20 and B2 phases from high P-T reactions between FeSi and H. (**a** and **b**) XRD patterns of the fresh and temperature-quenched samples at 42.6 and 57.5 GPa, respectively. (**c** and **d**) Decompression XRD patterns of the synthesized products from heating at 46.1 and 61.9 GPa, respectively. The blue and red ticks indicate the expected peak positions for the B20 and B2 phases, respectively. After heating up to 3500 K at 42.6 GPa, both the B20 and the B2 phases still exist, while after heating up to 2000 K at 57.5 GPa, only the B2 phase remains. A substantial decrease in peak widths found in **a** and **b** show that the samples were heated sufficiently for recrystallization and stress relaxation. The wavelength of the incident X-ray is 0.3344 Å.

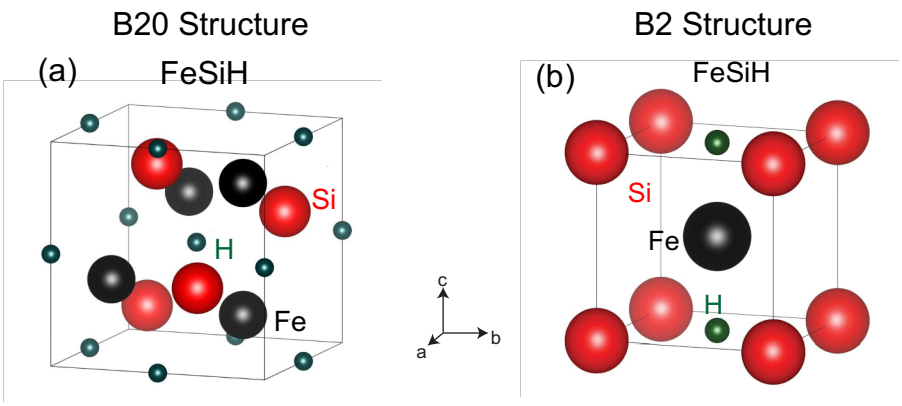

Figure S4: Additional crystal structure models considered for H alloying in the FeSi phases in this study. (**a**) The B20-structured FeSiH. (**b**) The B2-structured FeSiH. In **a**, H occupies the interstitial sites of all cubic centers. In **b**, H occupies 1/3 of the distorted octahedral interstitial sites.

Table S1: Parameters for the density functional theory calculations in this study. Encut: kinetic energy cutoff; *k* grids: Monkhorst-Pack *k*-point grids; Cells: Super-cell configuration.

Phases	**Encut (eV)**	***k* grids**	**Cells**
B20 FeSi	1200	6×6×6	1×1×1
B20 FeSiH	1200	6×6×6	1×1×1
B20 $FeSiH_{0.25}$	1200	6×6×6	1×1×1
B2 FeSi	1200	10×10×10	1×1×1
B2 FeSiH	1200	10×10×10	1×1×1
B2 Fe_8Si_7H	1200	12×12×12	2×2×2
B2 Fe_7Si_8H	1200	12×12×12	2×2×2

Table S2: Equation of state parameters for the B20 and B2 phases of FeSi and $FeSiH_x$ from our experiments and DFT calculations. Exp.: experiments; Str.: structure.

Str.	Method	Phase and reference	V_0 (Å^3)	K_0 (GPa)	K'_0
B20	Exp.	$FeSiH_x$ (this study)	92.5(2)	192(10)	5.8(10)
		FeSi (Knittle and Williams, 1995)	89.0(1)	209(6)	3.5(4)
		FeSi (Fischer et al., 2014)	90.4(1)	192.2(16)	5.03(17)
		FeSi (Lin et al., 2003)	90.2(1)	184.7(39)	4.75(37)
		FeSi (Guyot et al., 1997)	90.4(1)	172(3)	4
B20	DFT	FeSi (GGA, this study)	89.1	220.4	4.50
		FeSi (LDA, this study)	84.1	255.1	4.49
		FeSiH (GGA, this study)	98.1	206.5	4.40
		FeSiH (LDA, this study)	92.6	238.8	4.37
		$FeSiH_{0.25}$ (GGA, this study)	91.5	211.2	4.55
		$FeSiH_{0.25}$ (LDA, this study)	86.3	245.0	4.54
		FeSi (GGA, Caracas and Wentzcovitch, 2004)	90.2	221	4.18
		FeSi (LDA, Caracas and Wentzcovitch, 2004)	84.1	255	4.14
B2	Exp.	FeSi (this study)	21.4	208(8)	4
		FeSi (Fischer et al., 2014)	21.3	230.6(18)	4.17
		FeSi (Ono, 2013)	21.3	225(2)	4
		FeSi (Sata et al., 2010)	21.4	221.7(32)	4.17(6)
B2	DFT	FeSi (GGA, this study)	21.3	234.4	4.53
		FeSi (LDA, this study)	20.1	275.1	4.53
		Fe_7Si_8H (GGA, this study)	21.0	220.4	4.47
		Fe_7Si_8H (LDA, this study)	19.8	259.1	4.42
		Fe_8Si_7H (GGA, this study)	20.8	219.9	4.53
		Fe_8Si_7H (LDA, this study)	19.5	271.8	4.34
		FeSiH (GGA, this study)	26.3	168.6	4.44
		FeSiH (LDA, this study)	24.7	197.6	4.47

FeSi (GGA, Caracas and Wentzcovitch, 2004)	21.4	220	4.55
FeSi (LDA, Caracas and Wentzcovitch, 2004)	19.6	262	4.80
FeSi (GGA, Zhao et al., 2011)	21.6	199	4.78

References

Caracas, R., Wentzcovitch, R., 2004. Equation of state and elasticity of FeSi. Geophysical Research Letters 31.

Fischer, R.A., Campbell, A.J., Caracas, R., Reaman, D.M., Heinz, D.L., Dera, P., Prakapenka, V.B., 2014. Equations of state in the Fe-FeSi system at high pressures and temperatures. Journal of Geophysical Research: Solid Earth 119, 2810-2827.

Guyot, F., Zhang, J., Martinez, I., Matas, J., Ricard, Y., Javoy, M., 1997. PVT measurements of iron suicide (ε-FeSi) Implications for silicate-metal interactions in the early Earth. European Journal of Mineralogy, 277-286.

Knittle, E., Williams, Q., 1995. Static compression of ε-FeSi and an evaluation of reduced silicon as a deep Earth constituent. Geophysical Research Letters 22, 445-448.

Lin, J.F., Campbell, A.J., Heinz, D.L., Shen, G., 2003. Static compression of iron-silicon alloys: Implications for silicon in the Earth's core. Journal of Geophysical Research: Solid Earth 108.

Moroni, E., Wolf, W., Hafner, J., Podloucky, R., 1999. Cohesive, structural, and electronic properties of Fe-Si compounds. Physical Review B 59, 12860.

Ono, S., 2013. Equation of state and elasticity of B2-type FeSi: Implications for silicon in the inner core. Physics of the Earth and Planetary Interiors 224, 32-37.

Sata, N., Hirose, K., Shen, G., Nakajima, Y., Ohishi, Y., Hirao, N., 2010. Compression of FeSi, Fe3C, Fe0. 95O, and FeS under the core pressures and implication for light element in the Earth's core. Journal of Geophysical Research: Solid Earth 115.

Vocadlo, L., Price, G.D., Wood, I., 1999. Crystal structure, compressibility and possible phase transitions in ε-FeSi studied by first-principles pseudopotential calculations. Acta Crystallographica Section B: Structural Science 55, 484-493.

Zhao, K., Jiang, G., Wang, L., 2011. Electronic and thermodynamic properties of B2-FeSi from first principles. Physica B: Condensed Matter 406, 363-367.